

## Velocity and VTI anisotropy scanning in multicomponent seismic data

Christopher O. Ogiesoba<sup>\*</sup>, James E. Gaiser<sup>\*\*</sup>, and Robert R. Stewart<sup>\*</sup>

### ABSTRACT

We present a prestack method that scans for the average vertical-velocity ratio  $\gamma_0$ , and the effective anisotropic parameter  $\eta$ , using a new converted-wave (PS) non-hyperbolic traveltime equation. We tested our method using a numerical data set generated in ANIVEC (a frequency-wave number modeling package). The procedure entails computing semblance as a function of three variables: the PS velocity  $V_{ps}$ ,  $\gamma_0$ , and  $\eta$ . Results are displayed in 3D plots as a function of the PS zero-offset time  $t_{ps0}$ . We observe that the derived equation is valid for an offset-depth ratio of up to 1.5 for the tested model. There is a tradeoff in resolving  $\eta$  and the velocity ratio  $\gamma_0$  since both parameters control far offset moveout. The accuracy of the scanning technique increases with depth. It is inaccurate at shallow depths where the offset-depth ratio is greater than 1.5. At deeper levels, where the offset-depth ratio is 1 to 1.5, the errors in scanned velocity ratio  $\gamma_0$  and effective anisotropic parameter  $\eta$ , range from +9 to +10% and +0.2 to +8%, respectively.

### INTRODUCTION

The vertical velocity ratio, generally referred to as  $\gamma_0$ , plays a strategic role in multi-component data processing and interpretation. Some vertical transverse isotropic (VTI) parameters directly or indirectly depend on it, but how to recover it robustly from moveout analysis is not clear. One approach is the cross-correlation method developed by Gaiser (1996). This method can work well, but may fail where the P-wave and P-S have events of opposite polarity. Hence, there is the need to find an alternate prestack solution to the problem of P- and PS- wave correlation.

Thomsen (1999) showed that in VTI media, the PS moveout velocity is dependent on  $\gamma_0$  and  $\gamma_{eff}$  defined as the square of moveout velocity ratio divided by  $\gamma_0$ . He derived the converted-wave traveltime equation in VTI media. However, Thomsen's equation is complex and difficult to implement. To use Thomsen's equation for velocity analysis, it is necessary to modify his expression so that, the third term in the expression depends strictly on  $\gamma_0$ , and the effective anisotropic parameter  $\eta$ , and PS-wave moveout velocity. In this report, we show this modification and the application of the derived equation in scanning for the vertical velocity ratio and the effective anisotropic parameter.

<sup>\*</sup> CREWES Project, University of Calgary

<sup>\*\*</sup> WesternGeco, (Schlumberger), Denver, Colorado

This report presents the development and testing of a prestack method used to scan for the vertical velocity ratio ( $\gamma_0$ ), and the effective anisotropic parameter  $\eta$ , using the converted (PS) wave anisotropic (VTI) traveltime equations. The report focuses on the derivation of the anisotropic traveltime equation, parameter scanning code, model building, and application of the scanning method. The method outlined here is a prestack technique that uses moveout velocity analysis. It entails the computation of semblance as a function of three variables: the velocity ratio  $\gamma_0$ , PS moveout velocity  $V_{ps}$ , and  $\eta$ . Results are displayed in 3D as a function of the PS-wave zero-offset time  $t_{ps0}$ . By taking timeslices at various zero-offset times, maximum semblance will be displayed on the  $V_{ps}$ - $\gamma_0$  and  $\eta$ - $\gamma_0$  planes. The values of  $V_{ps}$ ,  $\eta$ , and  $\gamma_0$  associated with maximum semblance can then be identified.

### DERIVATION OF ANISOTROPIC TRAVELTIME EQUATION

According to Thomsen (1999) the PS traveltime equation can be written as,

$$t_{ps}^2(x) = t_{ps0}^2 + \frac{x^2}{v_{ps}^2} + \frac{A_4 x^4}{1 + A_5 x^2}, \quad (1)$$

where ,

$$A_4 = \frac{-(\gamma_0 - 1)^2}{4(\gamma_0 + 1)t_{ps0}^2 v_{ps}^4}, \quad (2)$$

and

$$A_5 = \frac{-A_4 v_{ps}^2}{\left(1 - \frac{v_{ps}^2}{v_{p2}^2}\right)} \quad (3)$$

where,  $v_{p2}$  and  $v_{ps}$  are respectively the P-wave and converted-wave rms velocities,  $\gamma_0$  is the average vertical velocity ratio  $v_p / v_s$ , and  $t_{ps0}$  is the converted-wave zero-offset time. Equation (1), though derived for single layered medium, it may also be used in multi-layered, isotropic and anisotropic media. However, the converted-wave velocity has expression which depends on the medium (Thomsen, 1999). In this regard, we need to find the right expression for the PS velocity and eliminate P-wave velocity from equation (3). By so doing, we will have converted-wave traveltime equation that only depends on converted-wave velocity and the vertical velocity ratio.

Thomsen (1999), shows that in anisotropic media (VTI), converted-wave velocity can be expressed as

$$v_{ps}^2 = v_{p2} \left( \frac{1 + \frac{1}{\gamma_{eff}}}{1 + \gamma_0} \right), \quad (4)$$

where,

$$\gamma_{eff} = \left( \frac{1 + 2\delta}{1 + 2\sigma} \right), \quad (5)$$

and where  $\sigma$  is the anisotropic parameter that controls the S-wave velocity.

Now from Thomsen and Tsvankin (1994),

$$\sigma = \gamma_0^2 (\varepsilon - \delta). \quad (6)$$

By substituting equation (6) in (5) and dividing numerator and the denominator by  $(1 + 2\delta)$ , (5) becomes:

$$\gamma_{eff} = \gamma_0 \left[ \frac{1}{\frac{1}{1 + 2\delta} + 2\gamma_0^2 \frac{(\varepsilon - \delta)}{(1 + 2\delta)}} \right].$$

This implies,

$$\gamma_{eff} = \gamma_0 \left[ \frac{1}{D + 2\gamma_0^2 \eta} \right], \quad (7)$$

where (Alkhalifah and Tsvankin, 1994)

$$\eta = \frac{(\varepsilon - \delta)}{(1 + 2\delta)}, \quad (7a)$$

and

$$D = \frac{1}{1 + 2\delta}.$$

From equation (7), we obtain:

$$1 + \frac{1}{\gamma_{eff}} = \frac{\gamma_0 + D + 2\gamma_0^2\eta}{\gamma_0}. \quad (8)$$

Substituting (8) in (4) leads to,

$$v_{ps}^2 = v_{p2}^2 \left[ \frac{\gamma_0 + D + 2\gamma_0^2\eta}{\gamma_0(1 + \gamma_0)} \right], \text{ or,}$$

$$v_{p2}^2 = \frac{v_{ps}^2 \gamma_0 (1 + \gamma_0)}{D + \gamma_0 (1 + 2\gamma_0\eta)}. \quad (9)$$

We can now find an expression for the converted-wave travetime in anisotropic media. Substituting (9) into (3), and the resultant into (1), we have

$$t_{ps}^2 = t_{ps0}^2 + \frac{x^2}{v_{ps}^2} - \left[ \frac{\frac{v_{ps}^2 (\gamma_0 - 1)^2 [\gamma_0^2 (1 - 2\eta) - D]}{D + \gamma_0 (1 + 2\gamma_0\eta)}}{\frac{4v_{ps}^2 [\gamma_0^2 (1 - 2\eta) - D] (\gamma_0 + 1) t_{ps0}^2 v_{ps}^4}{D + \gamma_0 (1 + 2\gamma_0\eta)} + \frac{(\gamma_0 - 1)^2 v_{ps}^4 (\gamma_0 + \gamma_0^2) x^2}{D + \gamma_0 (1 + 2\gamma_0\eta)}} \right] x^4$$

This expression reduces to

$$t_{ps}^2(x) = t_{ps0}^2 + \frac{x^2}{v_{ps}^2} - \left( \frac{(\gamma_0 - 1)^2 [\gamma_0^2 (1 - 2\eta) - D]}{4(\gamma_0^2 (1 - 2\eta) - D)(\gamma_0 + 1) t_{ps0}^2 v_{ps}^4 + (\gamma_0 - 1)^2 (\gamma_0^2 + \gamma_0) v_{ps}^2 x^2} \right) x^4 \quad (10)$$

where

$$D = \frac{1}{(1 + 2\delta)},$$

$$0 \leq D \leq 1, \text{ depending on } \infty \geq \delta \geq 0.$$

But if  $D=1$ , then we have

$$t_{ps}^2(x) = t_{ps0}^2 + \frac{x^2}{v_{ps}^2} - \left( \frac{(\gamma_0 - 1)^2 [\gamma_0^2 (1 - 2\eta) - 1]}{4(\gamma_0^2 (1 - 2\eta) - 1)(\gamma_0 + 1) t_{ps0}^2 v_{ps}^4 + (\gamma_0 - 1)^2 (\gamma_0^2 + \gamma_0) v_{ps}^2 x^2} \right) x^4 \quad (11)$$

Equation (11) is the anisotropic equation that was used in this project to perform the dual parameter scan for  $\gamma_o$  and  $\eta$ .

### How valid is equation (11)?

We tested the validity of the derived travetime equation by first creating model synthetic seismic records from ANIVEC. The models consist of a 4-layer anisotropic

media Table 1. The synthetic seismic records obtained are shown in Figure 1. To see how the synthetics generated using equation (11) compare with those from ANIVEC, we adopted the following procedure:

1. First generate a wavelet of dominant frequency, say 30Hz.
2. Compute traveltimes employing the derived equations and using the following parameters that were obtained from the models :
  - (a) zero offset-times  $t_{ps0}$  from the various layers,
  - (b) the  $v_{ps}$  associated with the layers,
  - (c) the velocity ratios and anisotropic parameters for each layer,
  - (d) and the offset values.
3. Next assign the wavelet amplitude to the computed traveltimes. Here, in this case, the wavelet amplitude represents the reflectivity (though this is not true).
4. Finally, plot the seismic traces.

The results of the above procedure are shown in Figures 2 and 3. Figure 3 shows the superposition of the traces from ANIVEC shown in green, over the traces generated using equation (11). The match is reasonable especially at shorter offsets.

Table1. The physical parameters used in constructing the model

Layer	Thickness	Vp(m/s)	Vs(m/s)	$\epsilon$	$\delta$	$\rho$ (gm/cc)
1	533	1600	400	0.137	-0.012	2.2
2	1300	4000	1428.6	0.036	-0.039	2.5
3	427	2700	900	0.170	0.000	2.3
4	1000	5500	2500	0.128	0.078	2.75

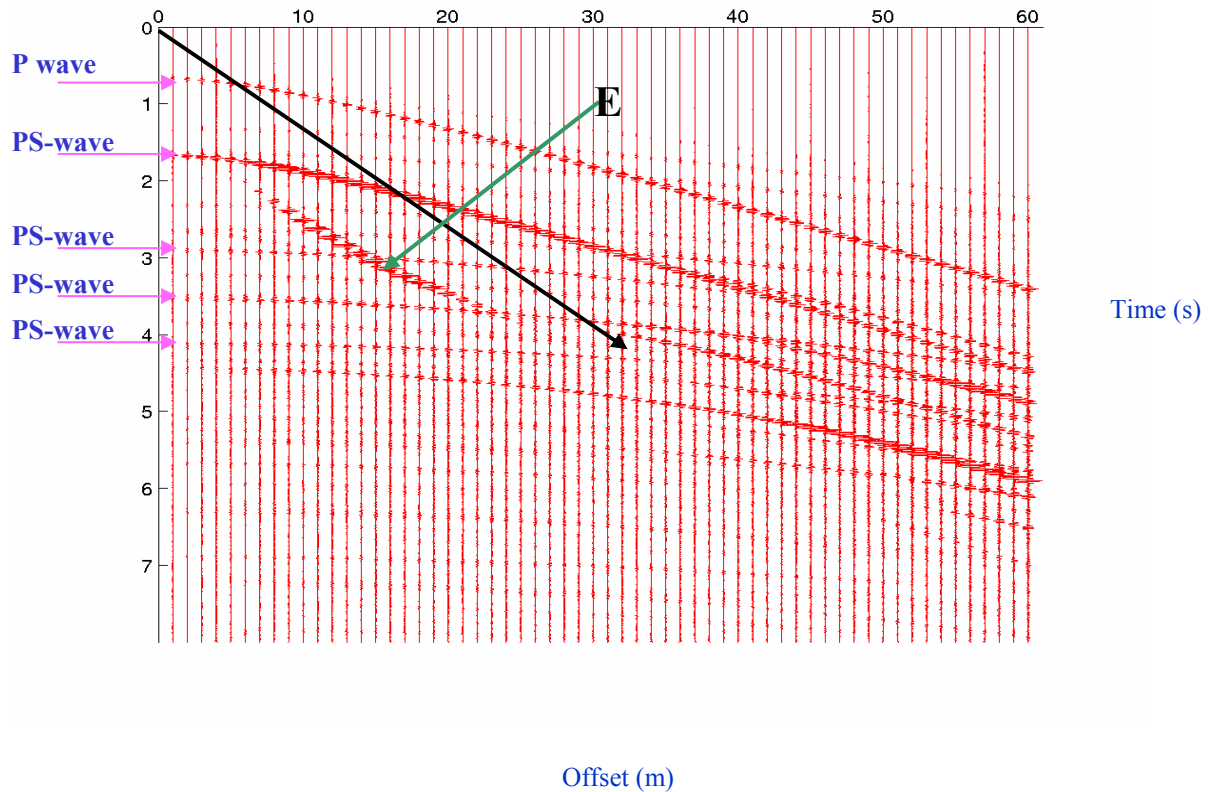


FIG. 1. Synthetic seismic record from ANIVEC modeling package; the event E appears to be a S-wave triplication from the shot. Horizon 1 is associated with large post-critical angle events which starts from 232.5m the far offsets at 6000m. Thus at this level, only two traces would meaningfully contribute to the velocity analysis at this level. The black arrow indicates where offset-depth ratio is equal to 1.

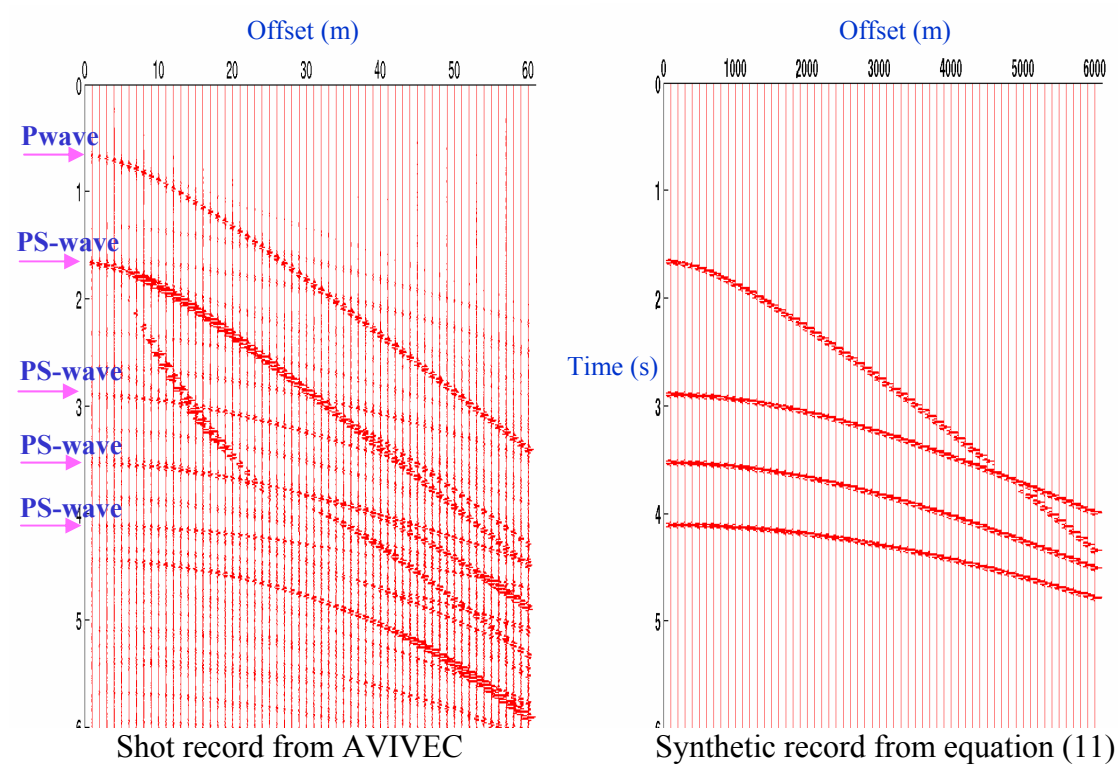


FIG. 2. In this figure are shown the shot record from ANIVEC modeling package, and the synthetic from equation (11) prior to the overlay.

### DEVELOPMENT OF $\gamma_0$ - $\eta$ SCANNING CODE

Having evaluated equation (11), we combined it with the Tanner and Koehler (1969) semblance expression, equation (12), to develop a semblance code. The objective of the code is to compute semblance as a function of PS velocity, velocity ratio  $v_p/v_s$ , and zero-offset two-way time; and then as a function of  $\gamma_0$ ,  $\eta$ , and zero-offset two-way time. Simply stated, the semblance coefficient is defined as the normalized output/input energy ratio, where the output trace is a simple compositing or sum of the input traces (Neidell and Tanner, 1971). Mathematically, the semblance coefficient SC can be stated as:

$$SC = \frac{\sum_{j=k-(N/2)}^{k+(N/2)} \left\{ \sum_{i=1}^M f_{i,j(i)} \right\}^2}{\sum_{j=k-(N/2)}^{k+(N/2)} \sum_{i=1}^M f_{i,j(i)}^2}, \quad (12)$$

where  $k$  is the time of the event calculated using the traveltime equation [in this case, equation (11)],  $N$  is the window length within which semblance is calculated,  $M$  is the number of traces,  $i$  is the channel (in this case the offset), and  $j$  is the time sample, and  $f_{i,j(i)}$  is the seismic amplitude at offset  $i$ , and at time sample,  $j$ . To execute the code

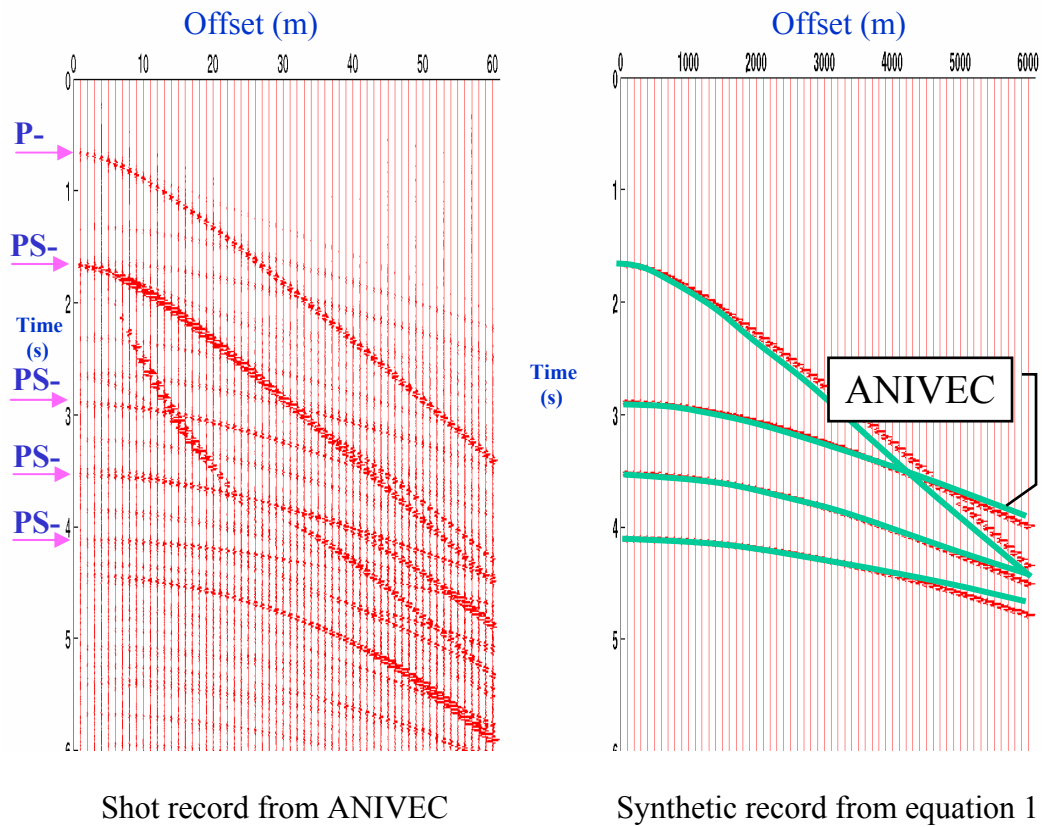


FIG. 3. This shows the comparison of the shot record from ANIVEC with the synthetic record from equation 11. The green curves are the digitized curves from ANIVEC shot record. Notice the almost perfect fit at near and intermediate offsets. Only the horizon 1 deviates significantly from the ANIVEC record.

a range of values of PS velocities,  $\gamma_0$ ,  $\eta$ , as a function of zero-offset traveltimes are scanned. In a manner akin to routine velocity analysis, values corresponding to maximum semblance are extracted.

### MODEL BUILDING

Model parameters for this exercise are shown in Table 1. The anisotropic parameters  $\epsilon$  and  $\delta$ , (Table 2) were taken from Thomsen (1986) and were used to compute the interval eta ( $\eta_{int}$ ) values; also, the interval stiffness  $c_{ij}$ , required by the modeling program were computed from these parameters. In computing the  $c_{ij}$ , we used the Thomsen (1986) formulas:



Table 2 . Shown in this table are the interval anisotropic parameters.

Layer	$\epsilon_{\text{int}}$	$\delta_{\text{int}}$	$\sigma_{\text{int}}$	$\gamma_{\text{int}}$	$\eta_{\text{int}}$
1	0.137	-0.012	2.3840	4.0	0.1527
2	0.036	-0.039	0.5880	2.8	0.0813
3	0.170	0.000	1.5480	3.0	0.1720
4	0.128	0.078	0.2420	2.2	0.0433

$$V_{p0} \equiv \sqrt{\frac{c_{33}}{\rho}}, \quad (12)$$

$$V_{s0} \equiv \sqrt{\frac{c_{55}}{\rho}}, \quad (13)$$

$$\epsilon \equiv \frac{c_{11} - c_{33}}{2c_{33}}, \quad (14)$$

$$\delta \equiv \frac{(c_{13} + c_{55})^2 - (c_{33} - c_{55})^2}{2c_{33}(c_{33} - c_{55})}, \quad (15)$$

$$\gamma \equiv \frac{c_{66} - c_{55}}{2c_{55}}. \quad (16)$$

We computed the interval  $\eta_{\text{int}}$  from equation (7a) [Alkhalifah and Tsvankin (1994),

Table 3 The average effective anisotropic parameters and  $\gamma_0$ 

Layer	$\delta_{\text{eff}}$	$\sigma_{\text{eff}}$	$\gamma_0$	$\eta_{\text{eff}}$
1	-0.0120	2.3840	4.0	0.1527
2	-0.0335	0.5274	3.41	0.1942
3	0.0000	0.2424	3.33	0.1936
4	0.0338	0.1221	3.10	0.1734

The computed stiffness coefficients from the above formulas are shown in Table 4. We assume the anisotropic parameter  $\gamma$  to be zero so that  $c_{55} = c_{66}$ .

Table 4. Shown in this table are the computed stiffness coefficients for individual layer

Layer	$\epsilon_{\text{int}}$	$\delta_{\text{int}}$	$\sigma_{\text{int}}$	$\gamma_{\text{int}}$	$\eta_{\text{int}}$
1	7.1752	4.8600	5.6320	0.3520	0.3520
2	42.8800	28.1990	40.0000	5.1022	5.1022
3	22.5348	13.0410	16.7670	1.8630	1.8630
4	104.4835	55.0101	83.1875	17.1875	17.1875

Furthermore, we employ the following Thomsen (1986) formulas to compute RMS velocities:

$$v_{prms}^2 = v_{p0}^2(1 + 2\delta), \quad (17)$$

and

$$v_{srms}^2 = v_{s0}^2(1 + 2\sigma), \quad (18)$$

where  $v_{p0}$  and  $v_{s0}$  are respectively P-wave and S-wave zero-offset velocities. Since  $\sigma$  is not initially known, we compute the value for each layer using (Thomsen and Tsvankin, 1994),

$$\sigma = \gamma_0^2(\epsilon - \delta). \quad (19)$$

Additionally, to obtain the effective value for each of the parameters, we use (Thomsen and Tsvankin, 1994),

$$\zeta_N = \frac{1}{v_{rms}^2 t_0} \sum_{i=1}^N v_{0i}^2 \zeta_i \Delta t_i, \quad (20)$$

where,  $\zeta_i$  stands for  $\delta_i$ ,  $\sigma_i$ , or  $\gamma_i$  (for the P-, SV-, or SH-wave, respectively) in each layer  $i$ , and  $\Delta t_i$  is the corresponding two-way vertical traveltime. Having found the P-, and S-wave RMS velocities, we then compute the converted-wave PS RMS velocities using Dix's formula as follows,

$$v_{psrms}^2 \sum_{i=1}^N t_{ps} = v_{prms}^2 \sum_{i=1}^N t_p + v_{srms}^2 \sum_{i=1}^N t_s. \quad (21)$$

The results from equations (17) to (20) are tabulated in Tables 5 and 6. Finally, to obtain the effective anisotropic parameter eta-effective ( $\eta_{\text{eff}}$ ), we employ Tsvankin (2001),

$$\eta(N) = \frac{1}{8} \left\{ \frac{1}{V_{nmo}^4(N)t_0(N)} \left[ \sum_{i=1}^N (V_{nmo}^{(i)})^4 (1 + 8\eta^{(i)})t_0^{(i)} \right] - 1 \right\} \quad (22)$$

where  $\eta(N)$  is  $\eta_{\text{eff}}$ ,  $V_{nmo}(N)$  is the P-wave moveout velocity,  $\eta^{(i)}$  is the interval eta, and  $t_0(i)$  is the two-way interval traveltimes. In computing P-wave  $V_{nmo}(N)$ , we use Dix's equation in line with Tsvankin (2001) recommendation.

Table 5. The P-, S-, and the PS-wave computed interval traveltimes, as well as the PS wave 2-way total traveltimes for each layer.

Layer	Vp0-int(m/s)	Vs0-int(m/s)	Tp0-int(s)	Ts0-int(s)	Tps0-int(s)	Tps0-2-way(s)	Vprms(m/s)	Vsrms(m/s)	Vpsrms(m/s)
1	1600	400	0.3333	1.3325	1.6655	1.6655	1581	961	1113
2	4000	1428.6	0.3250	0.9100	1.2350	2.9010	2685	1304	1718
3	2700	900	0.1581	0.4744	0.6325	3.5330	2685	1389	1775
4	5500	2500	0.1818	0.4000	0.5818	4.1150	3321	1527	2107

Table 6. Computation of  $\eta_{\text{eff}}$  using Table values and equation (22).

Layer	$\eta_{\text{int}}$	Tp0-int	Tp01-way total	Tp0 2-way int	Tp02-way total	Vp0(m/s)	Vprms(m/s)
1	0.1527	0.3333	0.3333	0.6666	0.6666	1600	1600
2	0.0813	0.3250	0.6580	0.6500	1.3160	4000	3032.7
3	0.1720	0.1581	0.8161	0.3162	1.6322	2700	2971.1
4	0.0433	0.1818	0.9979	0.3636	1.9958	5500	3567.9

The results obtained using equation (27) and the information in Table 6, are shown in Table 3. The computed PS RMS velocities, the effective eta, and the effective velocity ratios represent standards against which the scanned values of these parameters are compared.

### APPLICATION OF THE METHOD: $\eta-\gamma_0$ SCAN

Having validated the equation, built the model, generated synthetics and computed all the necessary parameters, we are now ready for the  $\eta-\gamma_0$  scan. In applying the algorithm, the following procedure is adopted;

1. First compute semblance as a function of  $\gamma_0$ ,  $V_{ps}$ , versus the zero-offset time,  $t_{ps0}$  assuming  $\eta$  to be zero in equation (11). Then obtain a 2D velocity semblance display, from which stacking velocity-time pairs are picked.
2. Next, interpolate velocities from the start to end of record time at the desired sampling rate.
3. Compute semblance as a function of  $\eta$ ,  $\gamma_0$ , versus  $t_{ps0}$  using the interpolated (and fixed)  $V_{ps}$  (PS stacking velocities) at corresponding times. This procedure will output a 2D  $\gamma_0$  function (semblance) display, from which  $\gamma_0$ - $t_{ps0}$  pairs are picked.
4. Display  $\eta$ ,  $\gamma_0$  and  $t_{ps0}$  semblance in 3D and obtain timeslice at picked times; from the timeslices i.e. from  $\eta$ - $\gamma_0$ -plane, obtain  $\eta$  values at corresponding  $\gamma_0$  values, that correspond to maximum semblance.

The results of the above processes are shown in Figures 4 to 9. Figure 4 shows the 2-D velocity semblance obtained from step (1). The red arrows indicate locations of velocity-time pairs corresponding to maximum semblance. These velocity-time pairs are interpolated for the  $\eta$ - $\gamma_0$  scan. In Figure 5 is shown the velocity ratio ( $\gamma_0$ ) semblance. The black arrows indicate the  $\gamma_0$ -time pairs corresponding to maximum semblance; while the red dots indicate the true (computed) values of  $\gamma_0$ . Apart from shallowest reflecting layer, results from the other horizons are in good agreement with the computed values; the maximum error being +10%.

Figures 6 to 9 show the three dimensional display of semblance. These figures show timeslice ( $\eta$ - $\gamma_0$ -planes), at the various reflecting layers. The red dots indicate true locations of  $\gamma_0$  and  $\eta$  correspondence; while the white circles indicate scanned locations of  $\eta$  and  $\gamma_0$  correspondence at maximum semblance. Apart from the horizon one, the others are in good agreement with the computed values. The scanned  $\eta$  value at horizon one agrees with the computed value. The maximum error in  $\eta$  is +8.6%; and this occurs at the deepest level where semblance broadens.

### **Error analysis**

The errors between the computed and the scanned values for the average vertical velocity ratios are tabulated in Table 7; while the errors in eta are shown in Table 8. From these Tables, it can be seen that apart from horizon 1, the maximum error in  $\gamma_0$  is 10%. The large error associated with horizon 1 is mainly due to the large post-critical angle events at this level.

Table 7. This table shows the errors between the computed  $\gamma_0^*$ , and the scanned  $\gamma_0^{**}$ . The \* indicates computed values, while the \*\* indicate scanned values.

Layer	$\gamma_{\text{int}}$	$\gamma_0^*$	$\gamma_0^{**}$	% Error in $\gamma_0$
1	4.0	4.0	2.75	-31
2	2.8	3.41	3.75	+10
3	3.0	3.30	3.60	+9
4	2.2	3.10	3.40	+9.7

Table 8. This table shows the errors between the computed  $\eta_{\text{eff}}^*$ , and the scanned  $\eta_{\text{eff}}^{**}$ . The \* indicates computed values, while the \*\* indicates scanned values.

Layer	$\eta_{\text{int}}$	$\eta_{\text{eff}}^*$	$\eta_{\text{eff}}^{**}$	% Error in $\eta_{\text{eff}}$
1	0.1527	0.1527	0.1535	0.5
2	0.0813	0.1942	0.1945	+0.2
3	0.1720	0.1936	0.1985	+0.5
4	0.0433	0.1734	0.1884	+8.6

## CONCLUSIONS

The derived traveltime equation is valid for offset-depth ratios up to 1-1.5 and its accuracy increases with depth. It is inaccurate at shallow depths where offset-depth ratio is more than 1.5. The described dual parameter scanning method provides a means of estimating both the vertical velocity ratio  $\gamma_0$ , and the effective anisotropic parameter  $\eta$  sequentially. At offset-depth ratios of 1-1.5, the observed maximum error in  $\gamma_0$  is +10%; while the error in  $\eta$  varies from + (0.2-8.6) %.

In general,  $\gamma_0$  can be scanned from 3D semblance computation using the non-hyperbolic moveout equation (15), but the accuracy is reduced due to vertical velocity heterogeneity. The PS moveout velocity  $V_{\text{ps}}$  is well resolved with near offset data. There is tradeoff in resolving  $\eta$  and  $\gamma_0$  since both parameters control far offset moveout; also, it seems that there is more sensitivity in  $\gamma_0$  than  $\eta$ . Furthermore, post-critical angle events are issues to contend with at shallow depths, where offset-depth ratios is more than 1.5; this could account for the large error (-31 %) associated with horizon 1.

Finally, the derived equation needs further refinement to be applicable at offset-depth ratios of more than 1.5.

### **ACKNOWLEDGEMENTS**

We would like thank WesternGeco, Denver, for providing the ANIVEC modeling package used in generating the numerical data sets; and the CREWES sponsors for their financial support

### **REFERENCES**

- Alkhalifah, T., and Tsvankin, I., 1994, Velocity analysis for transversely isotropic media: *Geophysics*, 60, 5, 1550-1566.
- Thomsen, L., 1986, Weak Anisotropy: *Geophysics*, 51, 1954-1966.
- Tsvankin, I. and Thomsen, L., 1994, Nonhyperbolic reflection moveout in anisotropic media: *Geophysics*, vol 59, 1290-1304.
- Thomsen, L., 1999, Converted-wave reflection seismology over inhomogeneous, anisotropic media: *Geophysics*, vol. 64, 678-690.
- Tsvankin, I., 2001, *Seismic signatures and analysis of reflection data in anisotropic media*: Pergamon publication.
- Tessmer, G. and Behle, A., 1988, Common reflection point data-stacking technique for converted waves: *Geophysical Prospecting* 36, 671-688.

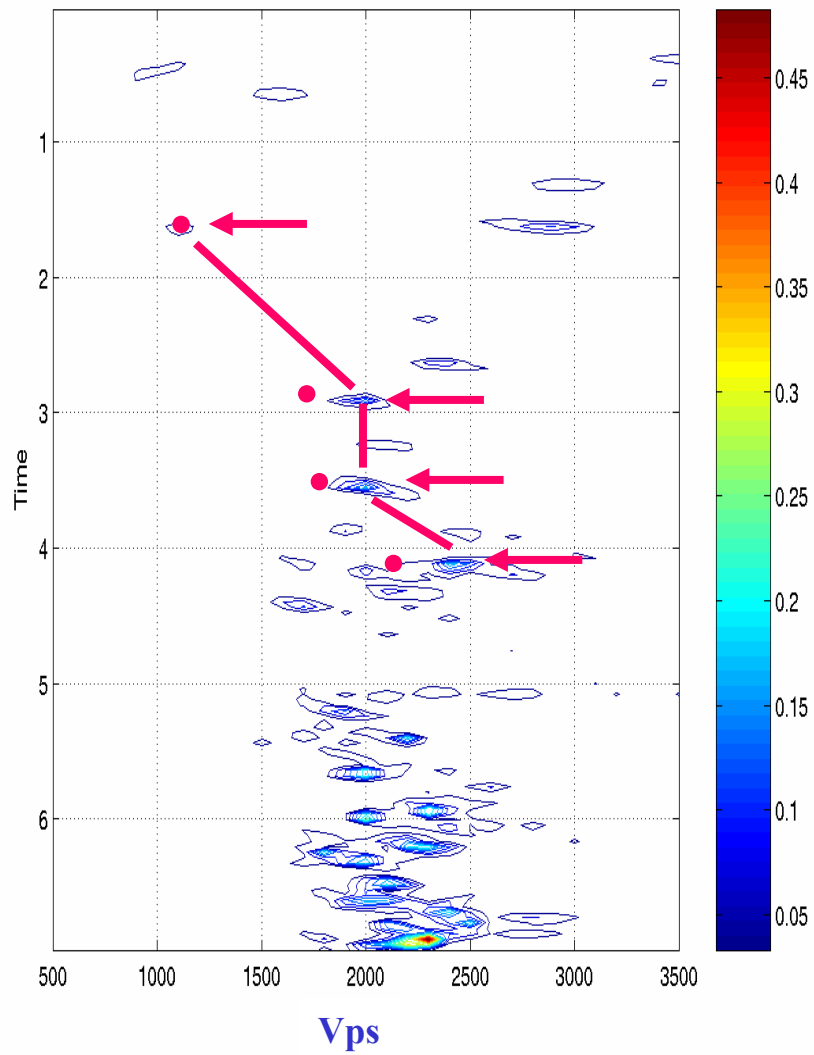


FIG. 4. 2-D display of semblance computed as a function  $\gamma_0$ ,  $V_{ps}$ , and the PS zero-offset time  $t_{ps0}$ . The red dots indicate computed  $\gamma_0$ - $t_{ps0}$  pairs; while the red arrows indicate the scanned  $V_{ps}$ - $t_{ps0}$  function.

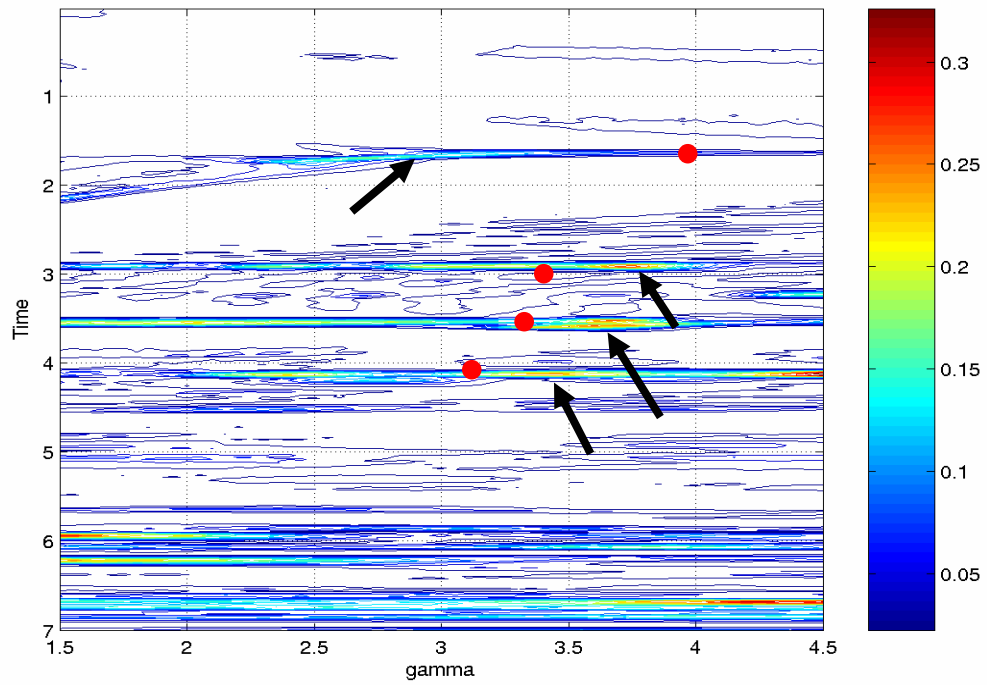


FIG. 5. 2-D display of semblance computed as a function  $\eta$ ,  $\gamma_0$ , and the PS zero-offset time  $t_{ps0}$ . The red dots indicate computed  $\gamma_0$ - $t_{ps0}$  pairs; while the black arrows indicate the scanned  $\gamma_0$ - $t_{ps0}$  function. Apart from the first horizon, other horizon values trend along the computed values.



## Layer 1

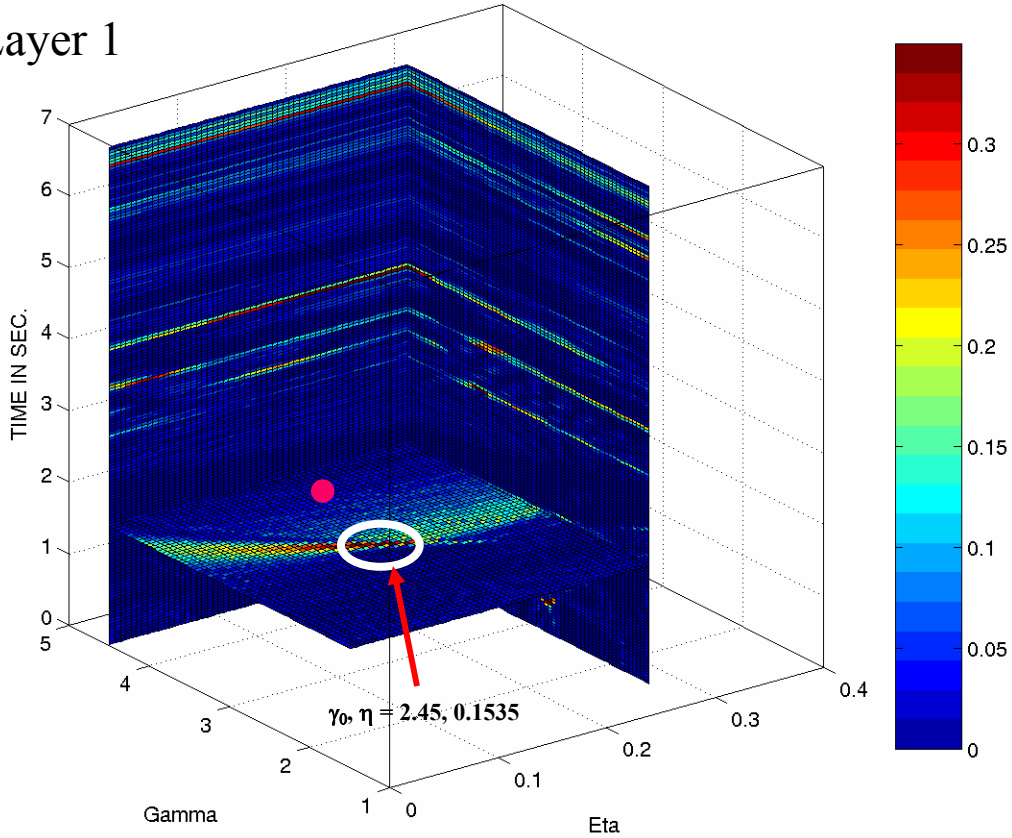


FIG. 6. The timeslice at 1.666 seconds; the red dot indicates location of the computed  $\gamma_0$  and  $\eta$  correspondence (location of maximum semblance); while the white circle shows the scanned location on the  $\eta$ - $\gamma_0$  plane. Computed location is  $(\gamma_0, \eta = 4, 0.1527)$ ; the scanned location is given by,  $(\gamma_0, \eta = 2.45, 0.1535)$ .

## Layer 2

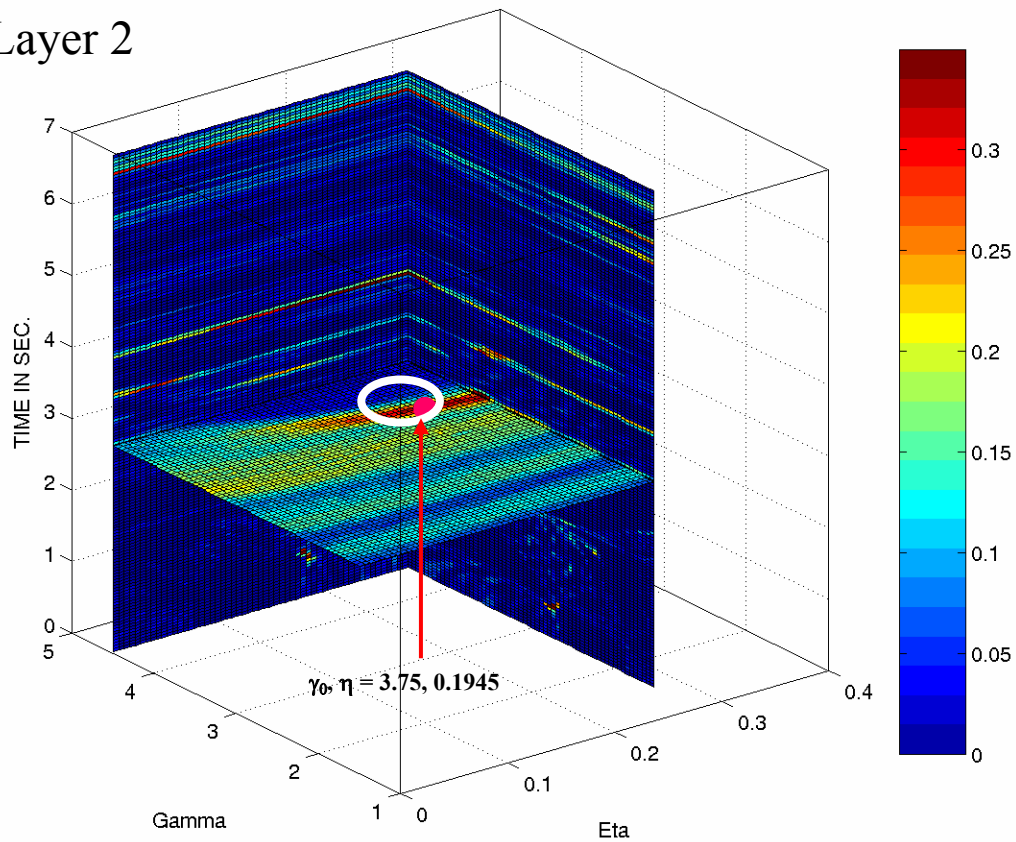


FIG 7. Timeslice at 2.900 seconds; the red dot indicates location of the computed  $\gamma_0$  and  $\eta$  correspondence (location of maximum semblance); while the white circle shows the scanned location on the  $\eta$ - $\gamma_0$  plane. Computed location is  $(\gamma_0, \eta = 3.41, 0.1942)$ ; the scanned location is given by,  $(\gamma_0, \eta = 3.75, 0.1945)$ .

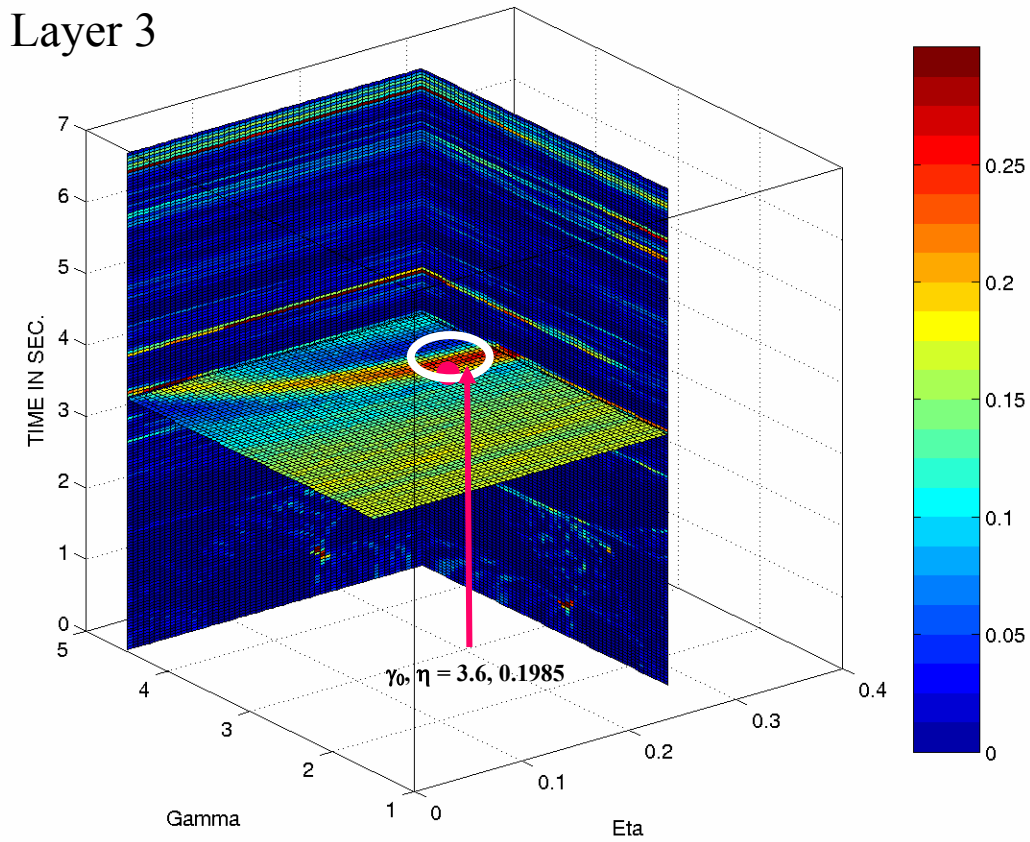


FIG 8. Timeslice at 3.533 seconds; the red dot indicates location of the computed  $\gamma_0$  and  $\eta$  correspondence (location of maximum semblance); while the white circle shows the scanned location on the  $\eta$ - $\gamma_0$  plane. Computed location is  $(\gamma_0, \eta = 3.3, 0.1936)$ ; the scanned location is given by,  $(\gamma_0, \eta = 3.6, 0.1985)$ .

### Layer 4

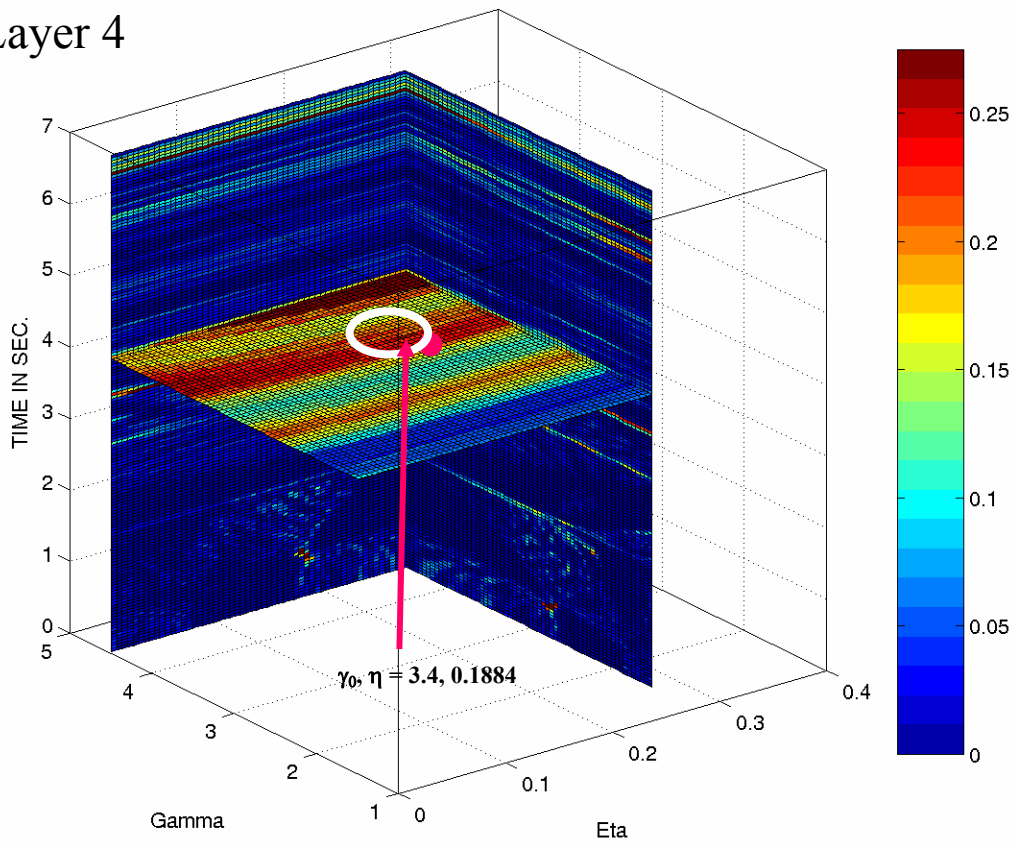


FIG 9. Timeslice at 3.533 seconds; the red dot indicates location of the computed  $\gamma_0$  and  $\eta$  correspondence (location of maximum semblance); while the white circle shows the scanned location on the  $\eta$ - $\gamma_0$  plane. Computed location is  $(\gamma_0, \eta = 3.1, 0.1734)$ ; the scanned location is given by,  $(\gamma_0, \eta = 3.4, 0.1884)$